Exploiting angular profiles signature for shape-based image classification and retrieval

Jamil Ahmad*

Department of Computer Science,
Islamia College,
Peshawar, Pakistan
Email: jamil.ahmad@icp.edu.pk
*Corresponding author

Khan Muhammad

College of Electronics and Information Engineering,
Sejong University, Seoul, South Korea
Email: khanmuhammad@sju.ac.kr

Zahoor Jan

Department of Computer Science,
Islamia College,
Peshawar, Pakistan
Email: zahoor.jan@icp.edu.pk

Abstract: Image classification and retrieval has significant importance in a wide variety of applications like object recognition, tracking, and content based retrieval, etc. Images usually consist of various objects which are segmented and then analysed for object-based classification and recognition. Owing to the absence of intensity and colour information, binary objects are difficult to recognise. They are usually represented using compact, geometrically invariant and robust features extracted from the object's contour or interior region. These features form the basis for recognition and govern the overall performance of classification systems. A new shape signature is introduced in this paper for representing shapes through angular profiles signature which are extracted from objects enclosed within minimum bounding circles. We have evaluated the discriminatory capabilities of this signature in shape recognition and retrieval on two shape datasets. Experimental results indicate that the signature is able to represent shapes effectively, achieving overall accuracy of 94%.

Keywords: angular profiles; shape signature; classification; descriptors.

Reference to this paper should be made as follows: Ahmad, J., Muhammad, K. and Jan, Z. (2016) 'Exploiting angular profiles signature for shape-based image classification and retrieval', *Int. J. Applied Pattern Recognition*, Vol. 3, No. 3, pp.276–292.

Biographical notes: Jamil Ahmad received his BCS in Computer Science from the University of Peshawar, Pakistan in 2008. He received his Masters in Computer Science with specialisation in image processing from Islamia College, Peshawar, Pakistan. Currently, he is pursuing his PhD in Digital Contents from Sejong University, Seoul, Korea. His research interests include image analysis, semantic image representation and content-based multimedia retrieval.

Khan Muhammad received his BCS in Computer Science from Islamia College, Peshawar, Pakistan in 2014 with research in image processing. Currently, he is pursuing his joint Masters-PhD in Digital Contents from Sejong University, Seoul, South Korea. His research interests include image processing, data hiding, steganography, watermarking, and video summarisation.

Zahoor Jan is currently an Assistant Professor in Computer Science at Islamia College Peshawar, Pakistan. He received his MS and PhD from FAST University Islamabad in 2007 and 2011, respectively. He is also the Chairman of the Department of Computer Science at Islamia College Peshawar, Pakistan. His areas of interests include image processing, machine learning, computer vision, artificial intelligence and medical image processing, biologically inspired ideas like genetic algorithms and artificial neural networks, and their soft-computing applications, biometrics, and solving image/video restoration problems using combination of classifiers using genetic programming.

1 Introduction

Shape classification is the task of assigning labels to unknown shapes based on their similarity with known shapes. Statistical classifiers are trained on sets of training objects using features extracted from the shapes. These features (signatures) are extracted either from the shape's boundary or interior region. An ideal shape descriptor offers greater intra-class similarity and lower inter-class similarity and is minimally affected by variations in size, orientation and position of the object in the image (Yang et al., 2008).

Shapes descriptors are categorised as contour-based and region-based. The first category uses only the boundary of a shape to extract features (Lee et al., 2010; Xu et al., 2009; Escalera et al., 2009; El-Ghazal, 2007; Qureshi et al., 2007), whereas, the second category uses the interior pixels of the shape to extract features (Zuva et al., 2012; Heikkilä et al., 2009; Liu et al., 2008). Both types have their strengths and weaknesses. The contour-based features are very sensitive to noise and boundary changes. On the other hand, region-based descriptors capture global features but ignore many interior shape details.

A shape signature is a one-dimensional function for compactly representing 2D shape areas or boundaries. They can be real valued as well as complex valued. A large number of shape signatures have been introduced in the past (Thai and Hoang, 2012; Chahooki and Charkari, 2013; Sajjanhar et al., 2008). Shape signature has been used as standalone features for shape-based representation and recognition. They have also been used for extracting Fourier or wavelet features.

Several methods for shape-based object representation have been presented in the past decade. Every signature analyses certain geometric characteristics of the shapes. The centroid distance function (CDF) measures the distance of each boundary point from the shape centroid, followed by Fourier transform (Gonzalez et al., 2009). CDF is invariant to translation by definition and scale invariance is achieved by feature normalisation. The chord length function (CLF) is also derived from the shape's contour. Unlike the CDF, it does not use any reference point, instead it computes distances between two boundary points a and b, given that the distance vector ab is perpendicular to the tangent vector at a (Zhang and Lu, 2005). In the angular function (AF), shape contour is represented as a 1D function of variations in the direction of the shape contour. These variations have significance to human visual system and therefore, may be used to represent object contours. The AF signature is sensitive to noise. This problem may be overcome through filtering prior to signature computation (Yang et al., 2008) however; it increases the computational expense of the signature. The triangular centroid area (TCA) signature computes the area of the triangles formed by nearby boundary points and the shape centroid. The areas of all such triangles yield the TCA signature (Zhang and Lu, 2005). A variation of the TCA is triangle area representation (TAR) shape signature. It forms triangles by taking all three points from the shape's boundary, followed by computing the areas of those triangles. For straight line segments, this area is zero. For convex contour fragments, it is positive and for concave fragments, it is negative (Yang et al., 2008). Complex coordinates (CC) signature is formed by the sequence of complex numbers obtained form the boundary. Farthest point distance (FPD) shape signature captures distances between shape corners. For a boundary point a, the FPD is computed as the distance between a and the farthest boundary point b. This distance is computed by adding distances between point a and the shape centroid c to the distance between points b and c.

Contour-based recognition methods has been more successful than the region-based methods and are therefore, investigated in more detail. This is due to the fact that human tends to discriminate shapes based on their contours. In Wang et al. (2012) a new contour-based shape signature was introduced. It was calculated by measuring the distances (heights) of sampled points of the outer shape boundary relative to a reference axis line. The points to one side of the reference line were considered as positive whereas points on the opposite sides were taken as negative. A dynamic programming approach was used for finding correspondence between points during the matching phase. The signature was evaluated on a number of shapes datasets and achieved a recognition rate of 90%. Felzenszwalb and Schwartz (2007) presented a hierarchical representation of shapes known as shape trees for capturing shape geometry at multiple levels of resolutions. A contour flexibility descriptor (CF) (Xu et al., 2009) was introduced by Xu et al. for representing deformable potential at each boundary point. Shape contexts (SC) (Belongie et al., 2002) tend to describe shapes by capturing landmark distributions in a set of 2D histograms, which allowed performed correspondence-based shape matching. SC was extended to inner distance shape context (IDSC) (Ling and Jacobs, 2007) in which the Euclidean distance was replaced with an articulation insensitive inner distance. From these approaches, it can be concluded that the contours carry significant information regarding structure of shapes which can be utilised for effective shape matching.

This paper presents angular profiles signature (APS) derived from the shape enclosed within the minimum bounding circle (MBC). The APS signature is tested as a standalone feature for retrieving similar shapes from a large dataset. Later in the paper, the performance of five different classifiers is thoroughly evaluated using the proposed signature for shape classification. Optimal set of values have been determined for all classification schemes. Experimental results reveal that the signature performs considerably well in representing and retrieving similar shapes. The experiments also confirm that a high degree of classification accuracy can be achieved with the proposed signature.

2 Materials and methods

This section presents the procedure for computation of the proposed APS followed by its characteristics.

2.1 Computation of the shape signature

The proposed signature is computed after enclosing the shape within an MBC. The MBC is the smallest circle that can contain a shape. The shape central point (centroid) is taken as the centre of the MBC and the point on the shape contour with max distance from the centroid is taken as its diameter. The algorithm for calculating the signature is explained below.

1. The centroid of the shape (cx, cy) is calculated that serves as the central point for the MBC. xi and yi are the x and y coordinates of the binary shape pixels.

$$\text{centroid} = \left\{ \begin{aligned} cx &= \frac{1}{N}\sum_{i=1}^{N} x_i \\ cy &= \frac{1}{N}\sum_{i=1}^{N} y_i \end{aligned} \right\} \tag{1}$$

2. The diameter D and orientation θ of the shape are determined.

3. Before signature computation, the shape is rotated by $-\theta$ degrees to align it to horizontal axis, that will help making the feature invariant to rotation. The rotation of the shape is performed through the rotation transformation.

$$\begin{bmatrix} xi' \\ yi' \end{bmatrix} = R(-\theta) \begin{bmatrix} xi \\ yi \end{bmatrix} \tag{2}$$

where $R(\theta)$ is the rotation matrix, xi' and yi' are the rotated pixel coordinates. The full form of the equation is:

$$\begin{bmatrix} xi' \\ yi' \end{bmatrix} = \begin{bmatrix} -\cos(\theta) & \sin(\theta) \\ -\sin(\theta) & -\cos(\theta) \end{bmatrix} \begin{bmatrix} xi \\ yi \end{bmatrix} \tag{3}$$

4 Take profiles from the binary shape at angles φ_i, where i is taken from the range [0 180], passing through the shape centroid from one point (p1) on the MBC to the opposite point (p2) on the boundary of the MBC. The number of shape pixels encountered along the straight path from p1 to p2 forming angle φ_i are counted and stored in $N\varphi_i$. This count is then used to calculate the probability of shape pixels along the angular profile at φ_i.

$$Desc_i = \frac{N\varphi_i}{D} \tag{4}$$

where $Desc_i$ is the i^{th} shape feature point taken at angle φ_i representing the probabilities of occurrence of shape pixels along the angular profile. Various increments for the range of angles were evaluated and an optimal increment value was selected for which the angular profiles were extracted. The number of angles chosen defines the descriptor size. It is usually noticed that choosing a very high feature size has computational cost whereas choosing a small feature size fails to properly capture all the important characteristics of a shape. Therefore it is imperative to select an optimal feature size.

Since the feature consists of probabilities, the feature is by nature invariant to scale. And the calculation of the signature relative to the shape centroid makes it invariant to rotation as well. The shape enclosed within the MBC along with its major-axis and diameter is shown in Figure 1(a). The angular profiles at various angles are illustrated in Figure 1(b).

Figure 1 (a) Shape enclosed within MBC (b) Angular profiles illustrated (see online version for colours)

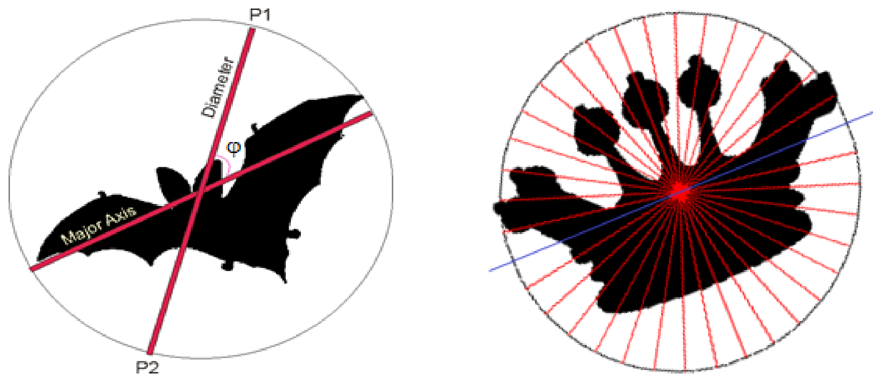

(a) (b)

2.2 Characteristics of the shape signature

A few properties of the proposed shape signature are presented in this section. We have already mentioned the invariance of the proposed signature to various geometric transformations. Here we show the feature invariance and discriminatory power of the descriptor with various shapes and also state how the signature is affected by shape deformation.

2.2.1 Feature invariance

The proposed shape signature is computed in such a way that it remains invariant to scale, position and orientation. A number of shapes with geometric transformation are given in Table 1. It can be seen that the signature remains unchanged during scale, orientation, and translation modifications.

Table 1 APS response to geometric transformations (see online version for colours)

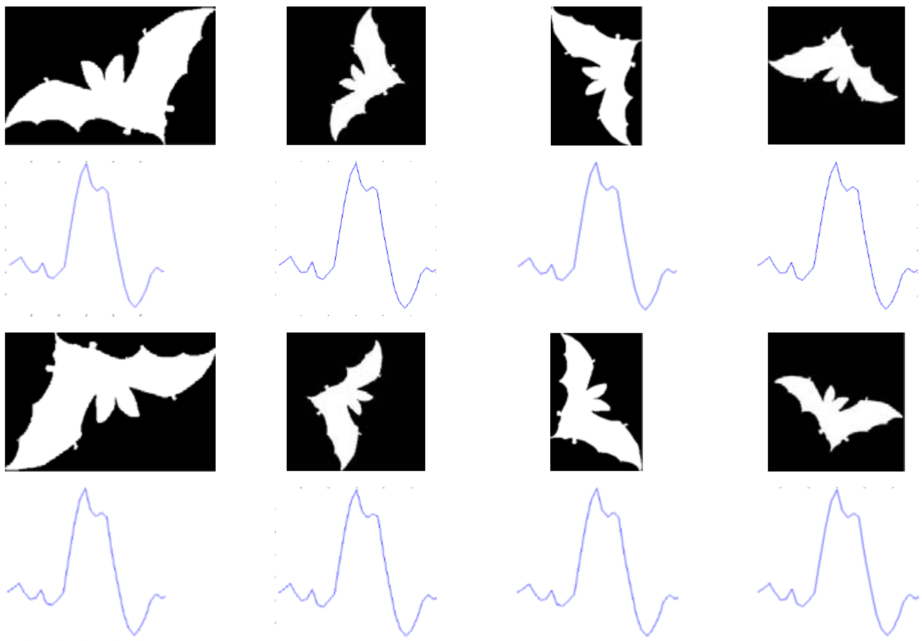

2.2.2 Discriminatory capability

A powerful shape descriptor tends to produce similar signatures for shapes belonging to same class and produces substantially different signatures for all other shapes (Zia-Uddin et al., 2014; Dubey and Jalal, 2015). Here we present signatures for similar classes as well as different classes for comparison. Table 2 shows the signatures for similar shapes as well as dissimilar shapes.

It is evident from the signatures in Table 2 that the proposed APS produces similar signatures for similar looking shapes and generates a different signature for all other shapes. The APS offers greater intra-class similarity and less inter-class similarity which is mostly the desirable property of such signatures. These characteristics exhibit the discriminatory capability of the signature. These characteristics help is shapes recognition and retrieval with a high degree of accuracy.

Table 2 APS for similar and dissimilar shapes (see online version for colours)

Shape (same class)	*Signature*	*Shape (different class)*	*Signature*
	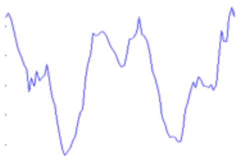		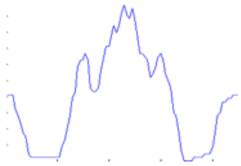
	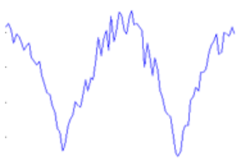		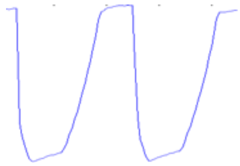
	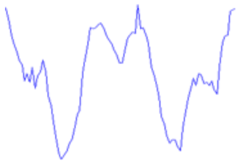		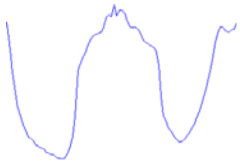
			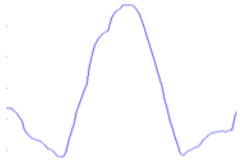
	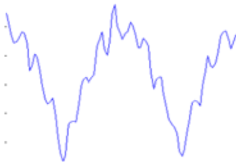		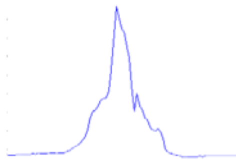
	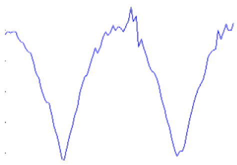		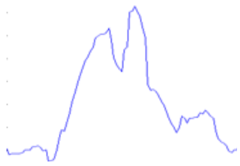

2.2.3 Response to shape deformation

The proposed signature has also been evaluated on shapes with varying degrees of deformations. As a result, minimal modifications were noticed in the signature. The resulting signatures in response to varying degrees of deformations are given in Table 3. The degree of deformation increases with every next shape. It can be observed that slight deformation along the shape contour minimally affects the APS. This property is desirable in recognition of slightly occluded objects.

Table 3 APS shape signatures in response to shape deformation (see online version for colours)

Shapes with increasing degree of deformation	*APS signature*	*Shapes with increasing degree of deformation*	*APS signature*

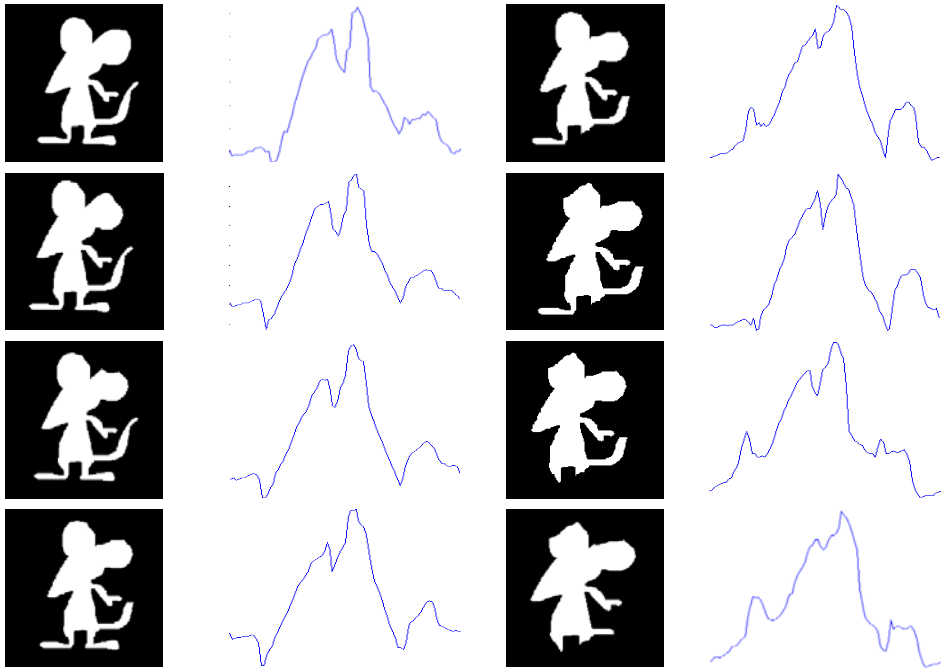

3 Results and discussion

The proposed shape descriptor's performance has been evaluated for shapes retrieval and classification. This section presents the dataset used, experimental setup, evaluation metrics and the results obtained by varying the APS size and classifier parameters.

3.1 Dataset

The MPEG-7 Part B and Kimia-99 shapes datasets were used for both retrieval and classification. MPEG-7 Part B dataset consist of 1,400 shapes organised into 70 classes where each class contains 20 images of an object with varying orientation, scale, and position. It is specifically designed to evaluate the performance of shape retrieval techniques (Ahmad et al., 2014) in the presence of such geometric transformations. Kimia-99 (Daliri and Torre, 2008) dataset is a relatively smaller dataset with 99 shapes organised into nine classes having 11 shapes in each class. Shapes in this dataset suffer from a greater degree of occlusions and deformations compared to MPEG-7 part B dataset. This dataset is used primarily to test the robustness of descriptor in the presence of occlusions, noise, and deformations. Furthermore, we introduced some further noise, and occlusions into the dataset to construct an extended version, so that the robustness of

APS to challenging scenarios can be assessed. The details of the experiments conducted and their results are given in the coming sections.

3.2 Evaluation metrics

For any classification problem, four general outcomes are usually considered. True positive (TP), true negative (TN), false positive (FP), and false negative (FN) that can be defined as:

TP classified correctly

TN classified incorrectly

FP rejected correctly

FN rejected incorrectly.

For the retrieval performance, as well as for measuring the classifiers' performance, accuracy has been used in this paper. This is measured as:

$$\text{Accuracy} = \frac{TP + TN}{TP + TN + FP + FN} \times 100 \tag{5}$$

3.3 Validation

For a dataset like the MPEG-7 part B containing more than a thousand shapes, *k*-fold cross validation has been used in these experiments. The value *k* is chosen to be 10. In *k*-fold cross validation, the entire dataset is divided into *k* parts. $k - 1$ parts are used for training the classifier whereas the k^{th} part is used for testing. In this way the classifier performance is evaluated across the entire dataset.

3.4 Shapes retrieval performance

The APS shape signature was evaluated as a standalone shape descriptor for retrieving similar shapes from the dataset. Results of some of the queries are shown in Table 3. The results show that the descriptor was able to retrieve similar looking shapes from the dataset which proves the discriminating ability of the proposed shape descriptor. It can be seen from the results in Table 3 that the shapes retrieved are similar in their appearance to the query shape. The descriptor performed well with most of the shapes. However for a certain number of shapes, especially the thin shapes, it could not perform well enough. For most of the shapes, the performance is summarised in Figure 2 with overall accuracy of 88%.

The shape retrieval evaluation was performed in MATLAB 7.14. The features extraction algorithm was implemented and tested on the said dataset using a GUI developed in MATLAB. For each query shape a number of relevant shapes were retrieved. A few of the query runs are depicted in Table 4. The results show that shapes with varying sizes, orientations and positions were retrieved successfully. Some of the shapes, however, were retrieved incorrectly but those shapes are mostly placed at lower ranks.

Figure 2 Shapes retrieval performance with the APS signature for various shapes (see online version for colours)

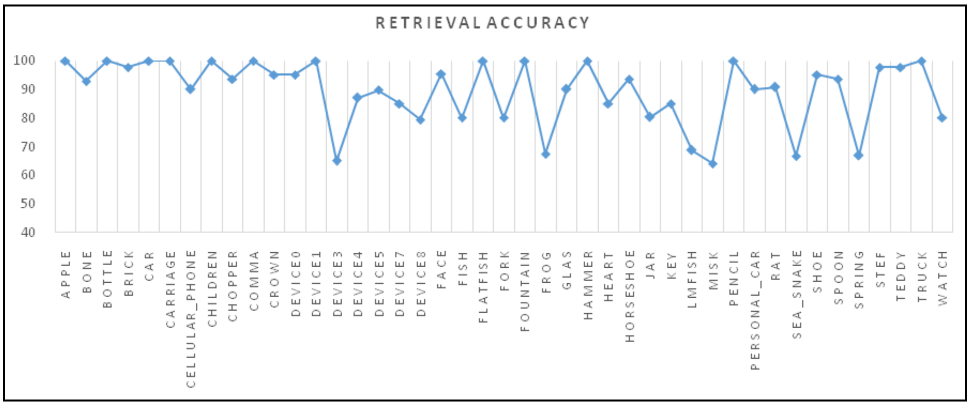

Table 4 Performance of KNN with different neighbourhood sizes

Neighbourhood size (k)	*Accuracy for varying feature sizes (%)*				
	45	*60*	*90*	*180*	*360*
1	93.5	93.7	93.7	94	93.5
2	87.85	88.5	88.42	90	88.5
3	87.71	88.14	87.5	89.2	88.14
4	86.2	86.5	85.7	88.3	86.14
5	86.2	86.42	86.2	88.3	88.14

3.5 Shape classification

The APS signature was also evaluated on five different classifiers from the machine learning family. All of the classifiers show promising results. However support vector machine (SVM) classifier performed the best. The rest of the classifiers used in these experiments were k-nearest neighbour (kNN), naïve Bayesian (NB), multilayer perceptron (MLP) and radial basis function network (RBFN). The performances of each of these classifiers along with the best set of parameters for each classifier are being investigated in this section.

3.5.1 K-nearest neighbour

The kNN classifier (Acharya and Ray, 2005) is a very simple classifier but it yields good classification accuracy. In order to assign a label to an unknown instance, it looks within its kNNs for the most dominant label and assigns that dominant label to it. The parameter *K* determines the size of the neighbourhood to be considered. The proposed APS signature was evaluated with different neighbourhood sizes. The results are given in Table 4.

3.5.2 Naïve Bayesian

NB is a famous supervised classifier used in pattern recognition applications. The Bayes 'decision theory' is the basis for this classifier whose decision principle is the selection of the most probable class. It assumes features independence within classes. However, it has shown considerable performance even if this independence is not valid (Duda et al., 2012). This classifier was tested with normal distribution and kernel density estimation and the results are given in Table 6. Overall classification accuracy achieved with the NB classifier was 86.8%.

Table 5 Shapes retrieval results using the angular profiles as a standalone descriptor

Query/ rank-1	*Rank-2*	*Rank-3*	*Rank-4*	*Rank-5*	*Rank-6*	*Rank-7*	*Rank-8*

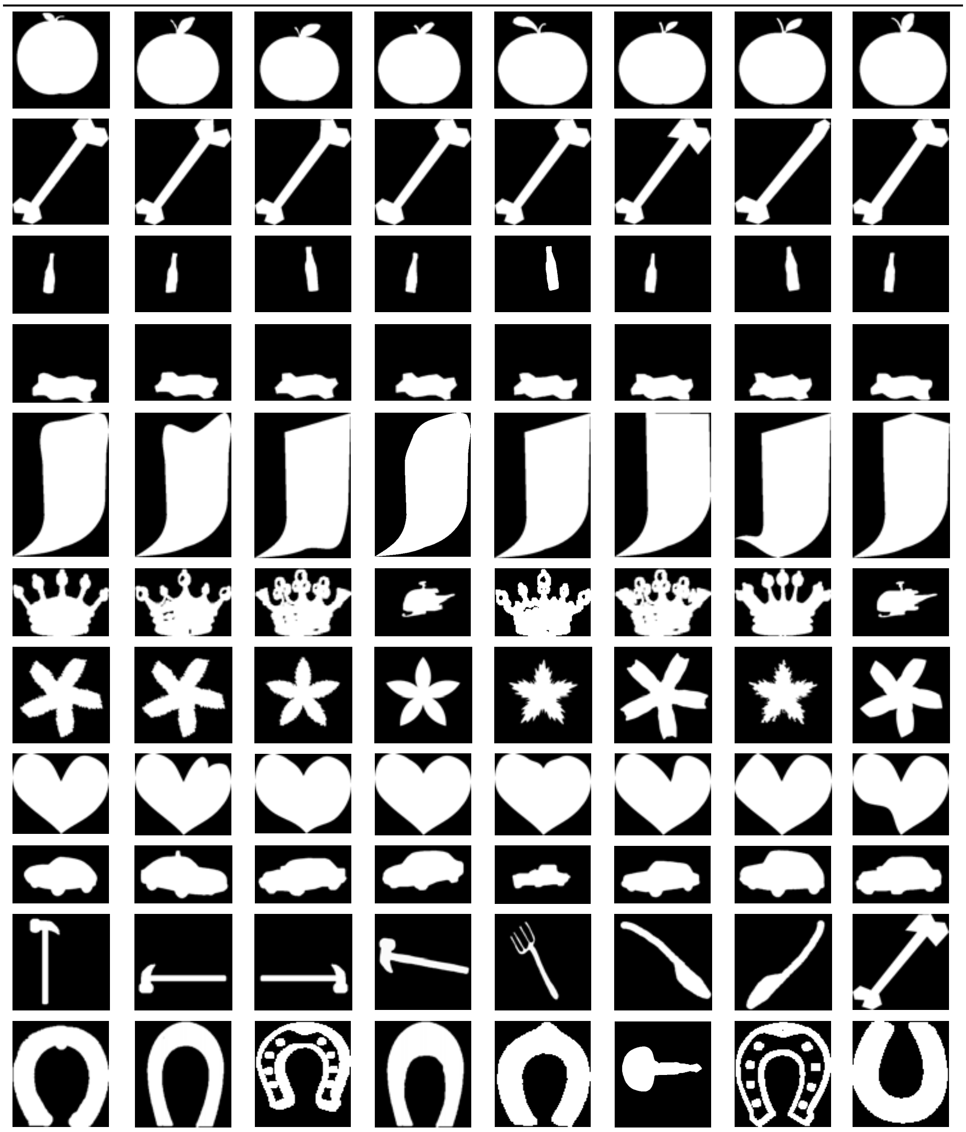

Table 6 Performance of NB with varying parameter values

Parameter setting	*Accuracy for varying feature sizes (%)*				
	45	*60*	*90*	*180*	*360*
Normal distribution	84	84.3	86.16	86.8	84.4
Kernel density estimation	83.5	83.14	86.16	85.8	83.1

3.5.3 *Multilayer perceptron*

MLP is an artificial neural network (ANN) capable of mapping inputs to appropriate outputs. A supervised learning algorithm called backpropagation is used for training this network (Alickovic and Subasi, 2011). We tested the performance of this classifier on our proposed shape signature by tuning the parameters learning rate α and momentum μ. The results are summarised in Table 7.

Table 7 Performance of MLP with varying parameter values

Learning rate (α)	*Momentum (μ)*	*Accuracy for varying feature sizes (%)*				
		45	*60*	*90*	*180*	*360*
0.3	0.2	89	93	91.8	93.2	93
0.3	0.3	90.1	93	91.5	92.0	92.2
0.4	0.2	90.3	93.1	90.6	92.6	92

3.5.4 *Radial basis function network*

RBFN is an ANN trained by the famous backpropagation algorithm. It has attracted researchers' attention in the recent years (Duda et al., 2012). It consists of two-layers of neurons with radial basis functions (RBF) as their activation functions. Training is performed through the least mean squares (LMS) learning algorithm which determines appropriate RBF weights. Table 8 shows the performance of RBFN classifier with the proposed signature.

Table 8 Performance of RBFN with varying parameter values

No. of clusters	*Min standard deviation*	*Accuracy for varying feature sizes (%)*				
		45	*60*	*90*	*180*	*360*
2	0.1	87.5	89.2	90	91.2	92
3	0.01	81.8	83.1	85.66	87	86.3
4	0.01	79.4	80	81.33	84.3	84.1

3.5.5 *Support vector machines*

SVMs were first introduced by Vapnikas binary classifiers (Rumpf et al., 2012; Ahmed et al., 2012; Ahmad et al., 2016). It uses a two-step classification process (Vapnik and Vapnik, 1998). In the first step a nonlinear mapping function (i.e., kernel function) is used to transform the input data from the feature space into a higher dimensional feature space. It facilitates the separation of nonlinearly separable data by transforming into linearly separable data at a higher dimension. During the second step, a maximum margin hyperplane is drawn as a decision boundary between the classes. The reason behind maximum separation is to allow prevention of misclassification of outliers. Different kernels and parameter values were tested with SVM. The results are shown in Table 9. In the first column the values in bracket represents the parameters. For polynomial kernel the value corresponds to the degree of the polynomial and for RBF kernel it corresponds to gamma. The polynomial kernel with degree 2 proved to be the best setup for SVM. It achieved 94% accuracy.

Table 9 Performance of SVM with various kernels

Kernel functions	*Accuracy for varying feature sizes (%)*				
	45	*60*	*90*	*180*	*360*
Polynomial kernel (1)	84.7	86.5	91.8	91.7	92.1
Polynomial kernel (2)	92	93.1	93.7	94	93
Polynomial kernel (3)	92.5	92.2	93.5	94	93
Polynomial kernel (4)	92.3	92.4	92.5	92.8	91.5
Polynomial kernel (5)	91.7	92.2	91.0	92	89.4
RBF kernel (0.2)	80.4	82	88.6	87.7	91.7
RBF kernel (0.4)	83.9	85	91.6	91.8	92.1
RBF kernel (0.6)	85.3	88.1	92.5	93.2	92.1
RBF kernel (0.8)	87.9	89.7	93.5	93	89.9
RBF kernel (1.0)	89.2	91.4	93.5	93.3	88.71

3.6 Robustness to noise and occlusions

In this experiment, we used the Kimia-99 dataset [as shown in Figure 3(a)] and the extended dataset [Figure 3(b)] to observe the effects of noise, occlusions, and geometric deformations. Results of the experiment conducted with the original dataset and extended dataset are summarised in Table 10. It can be seen that despite the relatively higher degree of occlusions, the shapes are represented effectively to be correctly classified using SVM. As a result of introducing further occlusions into the Kimia-99 dataset, overall recognition performance of the proposed method declined by 6%.

Table 10 Recognition rates using the Kimia-99 shapes dataset

Shape class	*Recognition rate (original)*	*Recognition rate (extended)*
	91%	87 %
	100%	92 %
	73%	66 %

Table 10 Recognition rates using the Kimia-99 shapes dataset (continued)

Shape class	*Recognition rate (original)*	*Recognition rate (extended)*
	82%	73 %
	100%	91 %
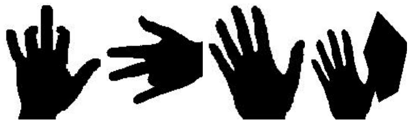	91%	84 %
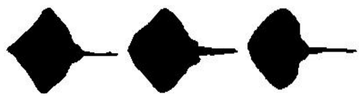	91%	87 %
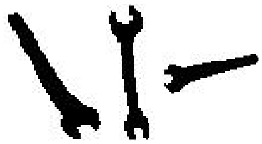	100%	92 %
	85 %	80 %
Overall accuracy	90%	84 %

Figure 3 Kimia-99 shapes dataset, (a) original (b) extended (sample)

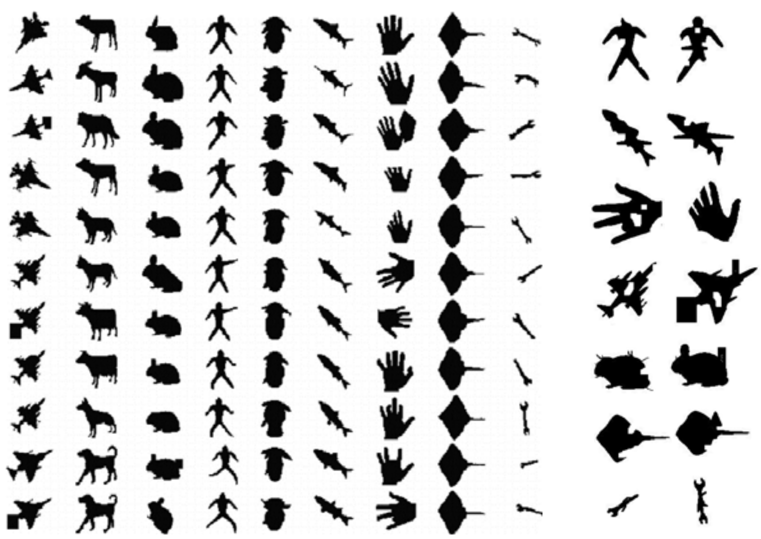

(a) (b)

3.7 Comparison with other shape signatures

The MPEG-7 part B shapes dataset has been extensively used by researchers to benchmark the performance of shape retrieval algorithms. Table 11 provides a brief summary and comparison of the proposed scheme with other existing classification methods for this dataset. Owing to its discriminatory capabilities, and robustness to partial occlusions, and noise, the proposed APS signature with SVM classifier is capable of recognising and retrieving similar shapes from a binary shapes dataset. Further study is needed to improve the performance of the proposed shape representation method to more efficiently cope with extensive shape deformations and noise.

Table 11 Classification rates for MPEG-7 dataset

Method	*Recognition rate (%)*
APS + SVM (proposed)	94.0
Triangle area representation (Alajlan et al., 2008)	87.23
IDSC (EMD) (Ling and Okada, 2007)	86.56
Symbolic representation (Daliri and Torre, 2008)	85.92
IDSC features (Ling and Jacobs, 2007)	85.40
Multiscale representation (Adamek and O'Connor, 2004)	84.93
Polygonal multiresolution (Attalla and Siy, 2005)	84.33
Farthest point distance (FPD) (El-Ghazal et al., 2009)	81.16
Curvature scale space features (Mokhtarian and Bober, 2011)	81.12

4 Conclusions

This paper presents APS to represent binary objects in images. Probabilities of occurrence of shape pixels are calculated from the profiles taken at various angles from objects enclosed within MBCs. The profiles are taken from one point on the MBC boundary to the opposite point passing through the MBC centre. APS was evaluated as a standalone feature retrieving similar shapes from a database. The results were good and for a high recall a precision of 88% was achieved. These figures can be improved further if it is used as a signature for Fourier descriptors or used in cascade with other features. Later in the paper, the performance of various classifiers was evaluated using the APS. Almost all of the classifiers performed well. SVM and KNN achieved high accuracies. The signature can be enhanced by adding new features to the signature computation like corners, curvatures, concavities and convexities. The authors left that for future research.

References

Acharya, T. and Ray, A.K. (2005) *Image Processing: Principles and Applications*, John Wiley & Sons, Hoboken, New Jersey, published simultaneously in Canada.

Adamek, T. and O'Connor, N.E. (2004) 'A multiscale representation method for nonrigid shapes with a single closed contour', *IEEE Transactions on Circuits and Systems for Video Technology*, Vol. 14, No. 5, pp.742–753.

Ahmad, J., Jan, Z., Uddin, Z. and Khan, S.M. (2014) 'A fusion of labeled grid shape Descriptors with weighted ranking algorithm for shapes recognition', *World Applied Sciences Journal*, Vol. 31, No. 6, pp.1207–1213.

Ahmad, J., Muhammad, K., Kwon, S.I., Baik, S.W. and Rho, S. (2016) 'Dempster-Shafer fusion based gender recognition for speech analysis applications', *International Conference on Platform Technology and Service (PlatCon)*, 15–17 February, pp.1–4.

Ahmed, F., Al-Mamun, H.A., Bari, A., Hossain, E. and Kwan, P. (2012) 'Classification of crops and weeds from digital images: a support vector machine approach', *Crop Protection*, Vol. 40, pp.98–104.

Alajlan, N., Kamel, M.S. and Freeman, G.H. (2008) 'Geometry-based image retrieval in binary image databases', *IEEE Transactions on Pattern Analysis and Machine Intelligence*, Vol. 30, No. 6, pp.1003–1013.

Alickovic, E. and Subasi, A. (2011) 'Data mining techniques for medical data classification', *The International Arab Conference on Information Technology*, Riyadh, Saudi Arabia.

Attalla, E. and Siy, P. (2005) 'Robust shape similarity retrieval based on contour segmentation polygonal multiresolution and elastic matching', *Pattern Recognition*, Vol. 38, No. 12, pp.2229–2241.

Belongie, S., Malik, J. and Puzicha, J. (2002) 'Shape matching and object recognition using shape contexts', *IEEE Transactions on Pattern Analysis and Machine Intelligence*, Vol. 24, No. 4, pp.509–522.

Chahooki, M.A.Z. and Charkari, N.M. (2013) 'Learning the shape manifold to improve object recognition', *Machine Vision and Applications*, Vol. 24, No. 1, pp.33–46.

Daliri, M.R. and Torre, V. (2008) 'Robust symbolic representation for shape recognition and retrieval', *Pattern Recognition*, Vol. 41, No. 5, pp.1782–1798.

Dubey, S.R. and Jalal, A.S. (2015) 'Fruit and vegetable recognition by fusing colour and texture features of the image using machine learning', *International Journal of Applied Pattern Recognition*, Vol. 2, No. 2, pp.160–181.

Duda, R.O., Hart, P.E. and Stork, D.G. (2012) *Pattern Classification*, John Wiley & Sons, Canada.

El-Ghazal, A., Basir, O. and Belkasim, S. (2007) 'A new shape signature for Fourier descriptors', *ICIP 2007*, IEEE.

El-Ghazal, A., Basir, O. and Belkasim, S. (2009) 'Farthest point distance: a new shape signature for Fourier descriptors', *Signal Processing: Image Communication*, Vol. 24, No. 7, pp.572–586.

Escalera, S., Fornés, A., Pujol, O., Radeva, P., Sánchez, G. and Lladós, J. (2009) 'Blurred shape model for binary and grey-level symbol recognition', *Pattern Recognition Letters*, Vol. 30, No. 15, pp.1424–1433.

Felzenszwalb, P.F. and Schwartz, J.D. (2007) 'Hierarchical matching of deformable shapes', *Conference on Computer Vision and Pattern Recognition, CVPR'07*, IEEE, pp.1–8.

Gonzalez, R.C., Woods, R.E. and Eddins, S.L. (2009) *Digital Image Processing Using MATLAB*, Gatesmark Publishing Knoxville, New Delhi, India.

Heikkilä, M., Pietikäinen, M. and Schmid, C. (2009) 'Description of interest regions with local binary patterns', *Pattern Recognition*, Vol. 42, No. 3, pp.425–436.

Lee, S-H., Bardunias, P. and Su, N-Y. (2010) 'A novel approach to shape recognition using the shape outline', *Journal of the Korean Physical Society*, Vol. 56, No. 3, pp.1016–1019.

Ling, H. and Jacobs, D.W. (2007) 'Shape classification using the inner-distance', *IEEE Transactions on Pattern Analysis and Machine Intelligence*, Vol. 29, No. 2, pp.286–299.

Ling, H. and Okada, K. (2007) 'An efficient earth mover's distance algorithm for robust histogram comparison', *IEEE Transactions on Pattern Analysis and Machine Intelligence*, Vol. 29, No. 5, pp.840–853.

Liu, Y., Zhang, D. and Lu, G. (2008) 'Region-based image retrieval with high-level semantics using decision tree learning', *Pattern Recognition*, Vol. 41, No. 8, pp.2554–2570.

Mokhtarian, F. and Bober, M. (2011) *Curvature Scale Space Representation: Theory, Applications, and MPEG-7 Standardization*, Springer Publishing Company Incorporated, Dordrecht, Netherlands.

Qureshi, R.J., Ramel, J-Y. and Cardot, H. (2007) 'Graph based shapes representation and recognition', in Escolano, F. and Vento, M. (Eds.): *Graph-Based Representations in Pattern Recognition*, Springer, Alicante, Spain.

Rumpf, T., Römer, C., Weis, M., Sökefeld, M., Gerhards, R. and Plümer, L. (2012) 'Sequential support vector machine classification for small-grain weed species discrimination with special regard to Cirsium arvense and Galium aparine', *Computers and Electronics in Agriculture*, Vol. 80, No. 1, pp.89–96.

Sajjanhar, A., Lu, G., Zhang, D. and Zhou, W. (2008) 'Corners-based composite descriptor for shapes', *Congress on Image and Signal Processing, 2008. CISP'08*, IEEE, pp.714–718.

Thai, V. and Hoang, S.T. (2012) 'Invariant pattern recognition using the RFM descriptor', *Pattern Recognition*, Vol. 45, No. 1, pp.271–284.

Vapnik, V.N. and Vapnik, V. (1998) *Statistical Learning Theory*, Wiley, New York.

Wang, J., Bai, X., You, X., Liu, W. and Latecki, L.J. (2012) 'Shape matching and classification using height functions', *Pattern Recognition Letters*, Vol. 33, No. 2, pp.134–143.

Xu, C., Liu, J. and Tang, X. (2009) '2D shape matching by contour flexibility', *IEEE Transactions on Pattern Analysis and Machine Intelligence*, Vol. 31, No. 1, pp.180–186.

Yang, M., Kpalma, K. and Ronsin, J. (2008) 'A survey of shape feature extraction techniques', in Yin, P-Y. (Ed.): *Pattern Recognition Techniques, Technology and Applications*, Chapter 3, pp.43–90, IN-TECH.

Zhang, D. and Lu, G. (2005) 'Study and evaluation of different Fourier methods for image retrieval', *Image Vis. Comput.*, Vol. 23, No. 1, pp.33–49.

Zia-Uddin, Z.J., Ahmad, J. and Abbasi, A. (2014) 'A novel technique for principal lines extraction in palmprint using morphological TOP-HAT filtering', *World Applied Sciences Journal*, Vol. 31, No. 12, pp.2010–2014.

Zuva, T., Olugbara, O.O., Ojo, S.O. and Ngwira, S.M. (2012) 'Object shape representation by kernel density feature points estimator', *First International Workshop on Signal and Image Processing (SIP 2012)*, Bangalore, India.